Supporting Information

Phase transition engineering for effective defect passivation to achieve highly efficient and stable perovskite solar cells

Dohyun Kim ‡[a], Hyuntae Choi ‡[a], Wooteak Jung ‡[a], Chanhyeok Kim [a], Eun Young Park [b], Sungryong Kim [a], Nam Joong Jeon *[b], Seulki Song *[c] and Taiho Park *[a]

a. *Department of Chemical Engineering, Pohang University of Science and Technology (POSTECH), 77 Cheongam-Ro, Nam-gu, Pohang, Gyeongbuk, Republic of Korea.*
E-mail: taihopark@postech.ac.kr

b. *Division of Advanced Materials Korea Research Institute of Chemical Technology (KRICT), Daejeon 34114, Republic of Korea*
E-maill: njjeon@krict.re.kr

c. *Department of Chemical Engineering and Applied Chemistry Chungnam National University, Daejeon 34134, Republic of Korea*
E-mail: sksong@cnu.ac.kr.

‡ These authors contributed equally.

* Corresponding authors

Contents

Fig. S20 Stabilized current density and power output of bare PSCs.

Fig. S21 *J-V* curve of best performing bare and DOFo-treated PSCs with different annealing temperatures.

Fig. S22 Histograms of device performance parameters of bare and DOFo-treated PSCs with different annealing temperatures.

Fig. S23 *J-V* curve of DOFo-treated PSCs with different DOFo concentrations.

Fig. S24 Histograms of device performance parameters of DOFo-treated PSCs with different DOFo concentrations.

Fig. S25 Light intensity dependent (a) V_{OC} and (b) J_{SC} of bare, as-deposited DOFo and liquid DOFo-deposited PSCs.

Fig. S26 (a) Equivalent circuit model for EIS measurement. (b) Nyquist plots of bare, as-deposited DOFo and liquid DOFo-deposited PSCs.

Fig. S27 *J-V* curves and best performing devices of (a) bare, (b) OAFo, (c) DAFo and (d) DOFo-treated PSCs using asy-PBTBDT HTL.

Fig. S28 Histograms of device performance parameters of bare and formate-treated PSCs using asy-PBTBDT HTL (10 devices each).

Fig. S29 Normalized device parameters of bare and AAFo-treated devices with time at the thermal conditions with (a) Spiro-OMeTAD based PSCs and (b) asy-PBTBDT based PSCs (85°C in N_2).

Fig. S30 Water contact angle of bare and AAFo-treated perovskite films.

Fig. S31 Water contact angle of DOFo-treated perovskite films with different annealing temperatures.

Fig. S32 Normalized device parameters of bare and AAFo-treated devices with time at the moisture condition with (a) Spiro-OMeTAD based PSCs and (b) asy-PBTBDT based PSCs (60±10 RH in RT).

Fig. S33 (a) Schematic illustration of the perovskite module. (b) Optical image of the perovskite module.

Table S1. Summarized PL decay components of bare and AAFo-treated perovskite before and after thermal stress (85℃ for 100 hours, N_2).

Table S2. Summary of V_{TFL} and n_{trap} of bare and AAFo-treated perovskite before and after thermal stress (85℃ for 100 hours, N_2).

Table S3. Summary of device performance parameters of best performing devices of bare and DOFo-treated PSCs with different annealing temperatures.

Table S4. The initial device performance parameters of bare and DOFo-treated PSCs with different annealing temperature (20 devices each).

Table S5. Summary of device performance parameters of best performing devices of DOFo-treated PSCs with different DOFo concentrations (10 devices each).

Table S6. The initial device performance parameters of DOFo-treated PSCs with different DOFo concentrations (10 devices each).

Table S7. Summary of calculated EIS parameters from Nyquist plots of bare and DOFo-treated PSCs with and without phase transition.

Table S8. Comparison of area, PCE and fill factor of small and large-area devices obtained in this work with those recently reported in literatures (planar PSCs with SnO_2 and Spiro-OMeTAD).

Experimental details

1) Materials

Zinc powder, 4-tert-butylpyridine (tBP), bis(trifluoromethane)sulfonimide lithium salt (Li-TFSI), hydrochloric acid (HCl), ethanol (EtOH), acetone (Ace), acetonitrile (AN), isopropanol (IPA), chlorobenzene (CB), chloroform (CF), dimethyl sulfoxide (DMSO), pottasium chloride (KCl) and dimethylformaide (DMF) were purchased from Sigma-Aldrich, formamidinium iodide (FAI), methylammonium bromide (MABr), methylammonium chloride (MACl) and cobalt(III) tris(bis(trifluoromethylsulfonyl)imide) (FK209) were purchased from Dyesol, lead (II) Iodide (PbI2) was purchased from TCI, lead(II) bromide (PbBr2) was purchased from Acros Organics and 2,2´,7,7´-tetrakis(N,N´-di-p-methoxyphenylamine)-9,9´-Spirobifluorene (Spiro-OMeTAD) was purchased from Merck.

2) Synthesis of alkylammonium formates

Formic acid (5 mL, 0.13 mol) was dissolved in dry ethyl ether and the solution was cooled to –16 °C under inert atmosphere and stirred for 1 hour. alkyllamines (0.13 mol) which dissolved in dry ethyl ether was slowly dropwise into the reaction media and keep the temperature of reaction media at –16 °C. After stirring for 2hours, the precipitated solid was collected by gravity filtration and washed using diethyl ether. The final products give the pure liquid or white solid.

3) Solar cell fabrication

Perovskite solar cells were fabricated on fluorine-doped tin oxide (FTO) coated glass substrates. The FTO coated glass substrates were etched using zinc powder and 2M hydrochloric acid (HCl). Then, they were rinsed with MUCASOL, deionized water (DI water), acetone, and isopropyl alcohol (IPA) by ultra sonication and then dried overnight. Tin oxide (SnO_2) compact layer was fabricated by sol-gel method. To breifly explain, solution 0.1M of $SnCl_2{\cdot}2H_2O$ in IPA is spin-coated at 4000 rpm for 30 then annealed at 190°C for 1 hour. UV-ozone is treated for 15 mins before the SnO_2 fabrication. After the SnO_2 formation, the ETL layer is UV-ozone treated and 1mg/ml of KCl in Di-water is spin-coated at 3000 rpm for 30s, and annealing at 100°C for 10 min. After cooling the substrate to room temperature, the substrates are treated with UV-ozone and transferred into drybox (relative humidity around 20% at 25°C). The perovskite precursor solution was prepared with the composition of FAI (1.4 M), PbI_2 (1.4 M), MABr (0.04 M), $PbBr_2$ (0.04 M) and MACl (0.5M) in DMF : DMSO = 8 :1 (volume ratio), and spin-coated in a two-step program at 1000 and 5000 rpm for 10 and 20 s. During the second step, 1000 μL of diethyl ether was gently poured on the substrate 10 s prior to the end of the program. Then the substrates were immediately annealed at 140°C for 15 mins. After annealing, 10mM of AAFo in CF (optimal concentration) is deposited dynamically under 5000rpm spin coating condition and annealed. Hole transport material solutions ((1) Spiro-OMeTAD: 72.3 mg Spiro-OMeTAD, 30.6 μL tBP, 19.5 μL LiTFSI (520 mg/mL in acetonitrile) in 1 mL chlorobenzene, (2) Asy-PBTBDT: 15mg/ml of asy-PBTBDT in chlorobenzene)was spin-coated at 5000 rpm for 30 s. Finally, electrode (100 nm for Ag and 80nm for Au) was thermally evaporated in high vacuum condition.

4) Device characterization

Using a Keithley 2400 SMU and an Oriel xenon lamp (450 W) with an AM1.5 filter, the solar cells were characterized in air under AM 1.5G illumination of 100 mW cm^{-2} (Oriel 1 kW solar simulator), which was calibrated with a KG5 filter certified by NREL. After light soaking for 1 minute, the current density-voltage (J-V) curves of all devices were measured by 30ms of scan time with 200 ms voltage settling time. The active area of device is 0.09 cm^2.

5) UV-vis measurement

The Ultraviolet-visible (UV-vis) absorption spectra were obtained using a Mecasys Optizen Pop UV-vis spectrophotometer for glass/perovskite with different light injection directions.

6) PL measurement Time-resolved photoluminescence (TRPL) mesurements

PL measurement Time-resolved photoluminescence (TRPL) mesurements were performed using time correlated single photon counting (TCSPC) system (HAMAMATSU/C11367-31). For TRPL measurements, a pulsed laser source was laser diode with a wavelength of 474 nm, a repetition rate of 100 kHz, fluence of ~ 4 nJ/cm2 and a pulse width of 70 ps. Steady state photoluminescence (PL) measurements were performed using the high resolution monochromator and hybrid photomultiplier detector (PMA Hybrid 40, PicoQuant GmbH). The TRPL and steady-state PL measurements were conducted using prepared samples: glass/perovskite or glass/ETL/perovskite or FTO/ETL/perovskite. The samples were excited from the glass side under ambient conditions with excitation wavelength of 474nm.

7) FTIR measurement

The Fourier transform infrared spectra of OAFo were measured using a Cary 600 spectrometer equipped with a MCT-A (mercury cadmium telluride) detector.

8) UPS measurement

The UPS measurements of the perovskites were performed at 4D PES beamline of PAL in Korea. The beam intensity used for the measurement were at 90eV, and the data were acquisted by kinetic swept mode.

9) SEM measurement

Field emission scanning electron microscope (FE-SEM, Hitachi S 4800) is used for SEM measurement for the perovskite layers.

10) SCLC measurement

The device structure and equation for trap density calculation are described in the manuscript. SCLC measurements were conducted using a Keithely 2400 SMU with voltage range from 0 V to 3V.

11) XRD measurement

X-Ray diffraction analysis of perovskite crystals were performed Rigaku D/Max-2200/PC wit he measurment range of 2° to 60° and 4°/s of scan speed.

12) XPS measurement

XPS measurements of the perovskites and pure OAFo is performed by ESCALAB 250 (Thermo Scientific) with 20eV of pass energy. Al K Alpha is used for the source gun and the spot size is 500μm.

13) IPCE measurement

For the IPCE measurement of PSCs, constant 100 W Xenon lamp source with an automated monochromator filters and 0.76 mm x 1.0 mm rectangular spot size was used (IQE-200B model).. The wavelength range for the measurement is from 300 to 900 nm.

14) EIS measurement

The electrical impedance of PSCs were measured by a computer-controlled potentiostat (SP-200, BioLogic).The Nyquist plot was measured in the frequency range of 1 MHz to 100 Hz under a bias of -0.9V in dark.

15) Confocal photoluminescence microscopy measurement

Confocal photoluminescence microsopcy images are taken using confocal laser scanning microscope (Leica TCS SP5). Acousto Optical Beam Splitter is used for emission splitting. HCX PL APO CS (63.0x1.30) GLYC 21°C UV objective and 476nm Ar laser is used for measurement.

16) Electroluminescence (EL) and Photoluminescence (PL) microscopy measurement

EL and PL measured by K3300 EPLI Solar Cell Imaging Test System. For EL, EL Powersource (±150V, 20A) was employed and for PL, 630nm Led was employed. Measurement conducted in dark room condition and motorized camera was used for imaging.

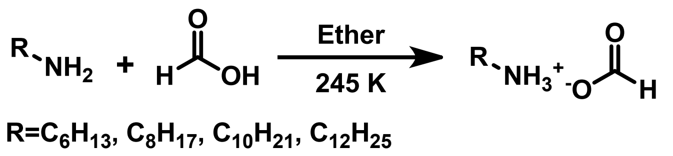

Fig. S1 The synthetic scheme of alkylammonium formate.

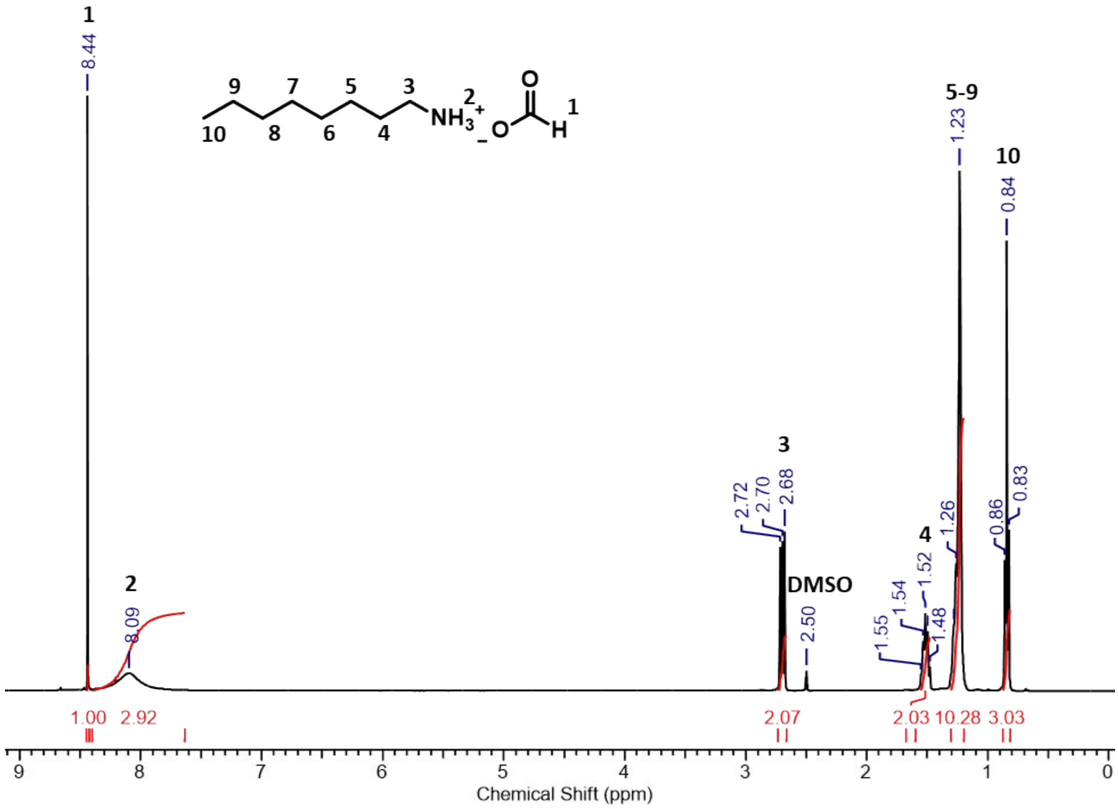

Fig. S2 ^{1}H NMR spectra of octylammonium formate.

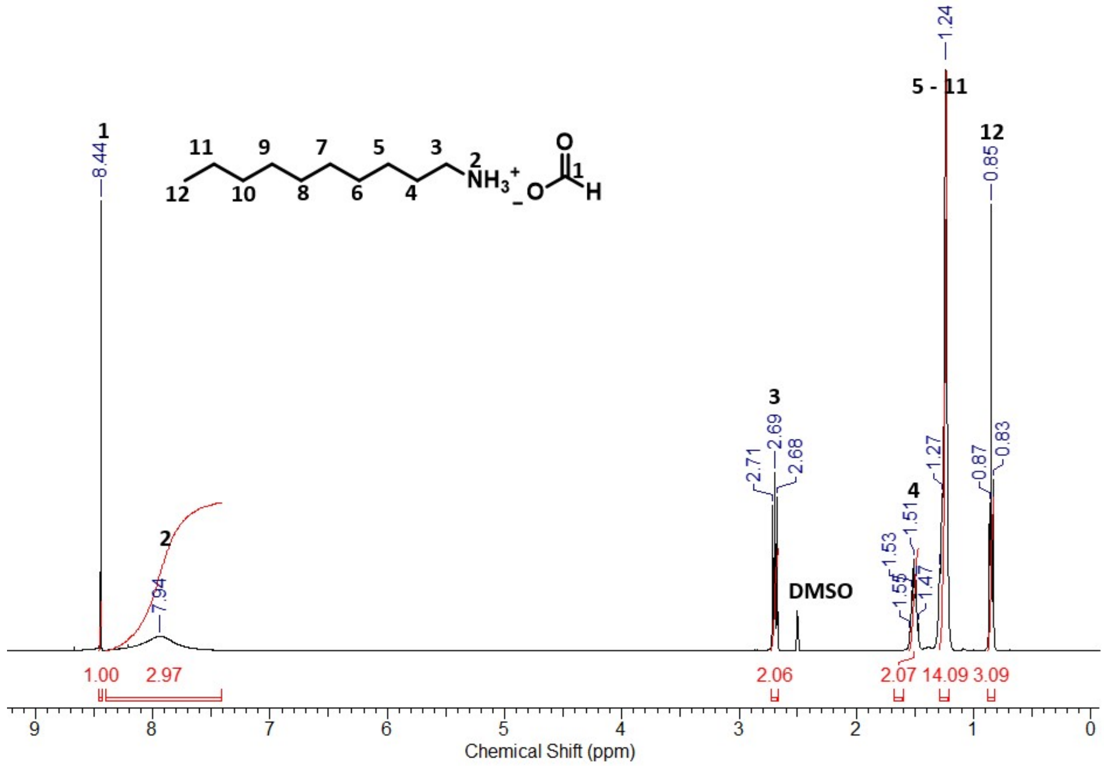

Fig. S3 [1]H NMR spectra of decylammonium formate.

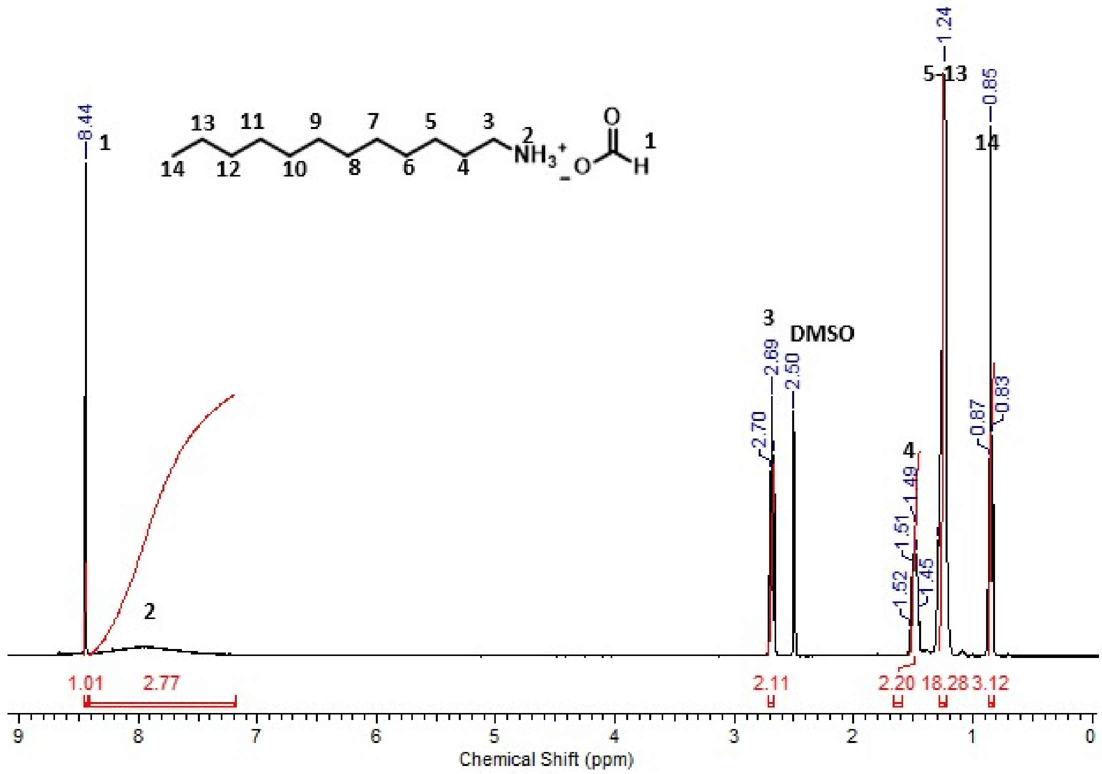

Fig. S4 ^{1}H NMR spectra of dodecylammonium formate.

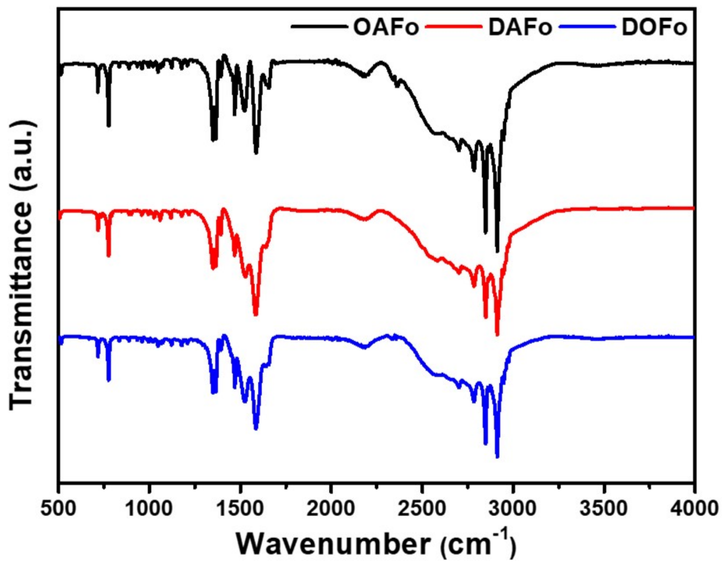

Fig. S5 FTIR data of alkylammonium formates.

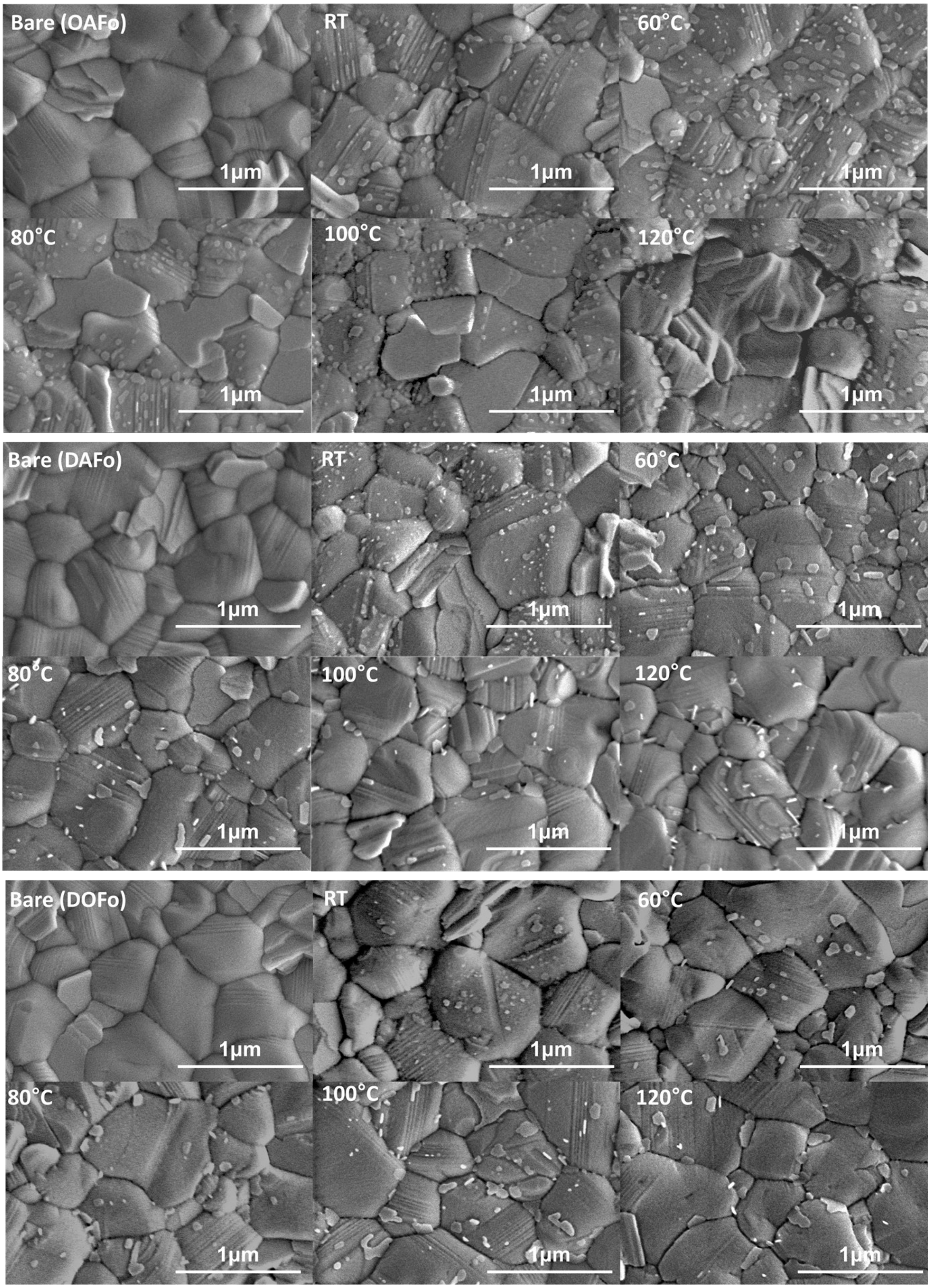

Fig. S6 SEM images of alkylammonium formate-treated perovskite films with different annealing temperatures (from room temperature to 120℃).

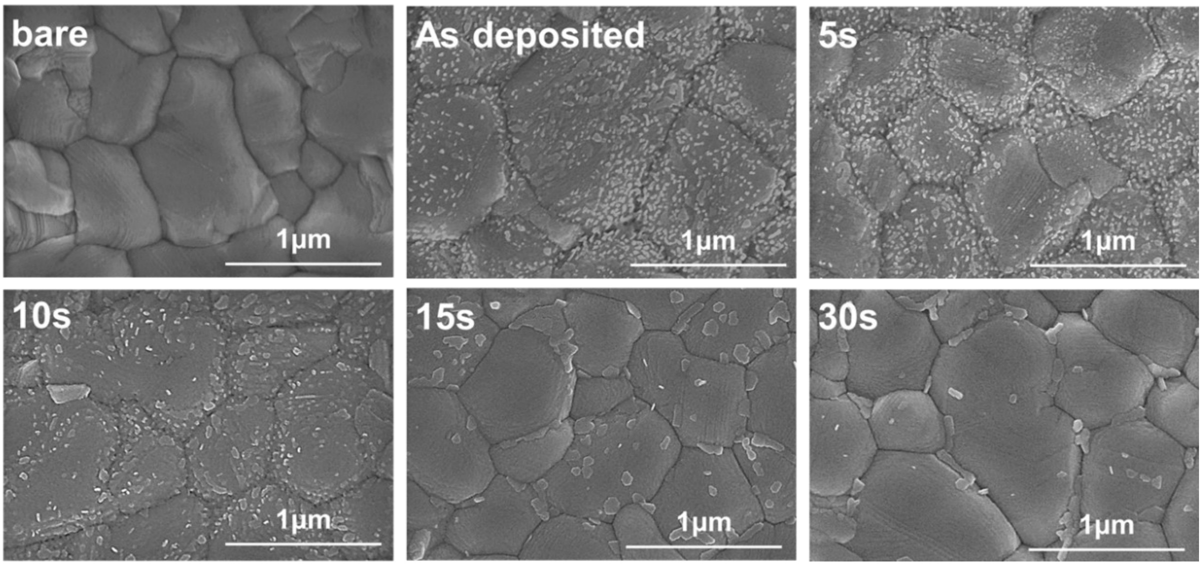

Fig. S7 SEM images of bare and DOFo-treated perovskite films with annealing time at 120℃.

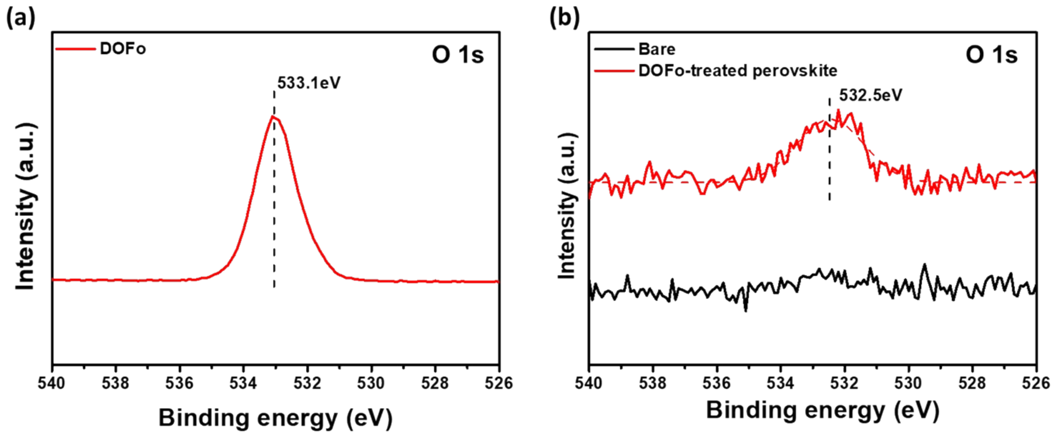

Fig. S8 XPS plots of (a) DOFo, (b) bare and DOFo-treated perovskite films at O 1s.

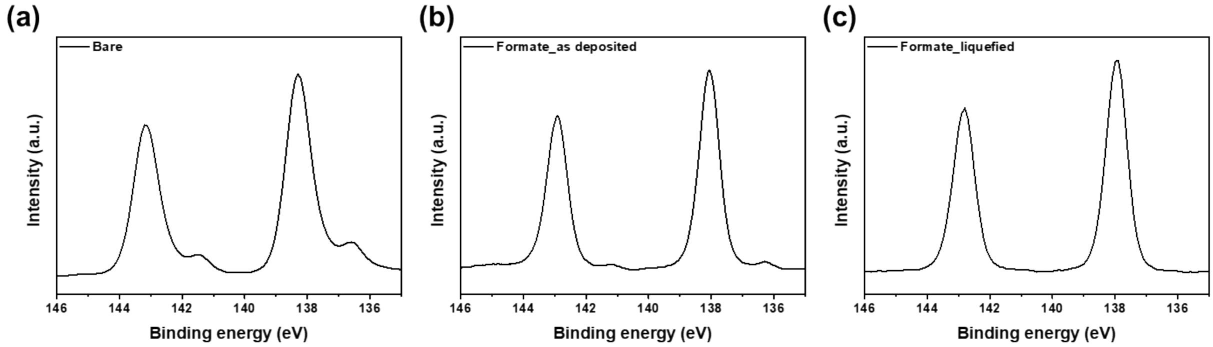

Fig. S9 XPS plots at Pb 4f of the (a) bare perovskite, (b) DOFo-treated perovskite and (c) DOFo-treated perovskite with liquefaction.

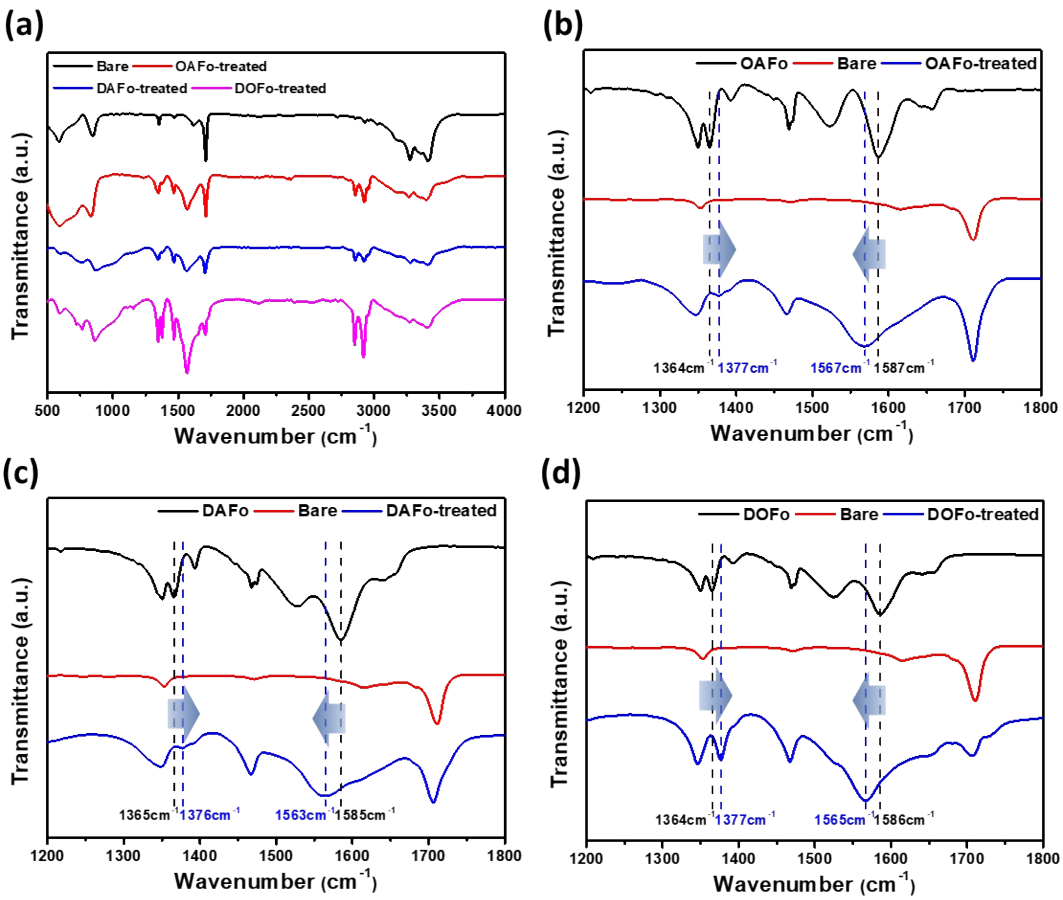

Fig. S10 FTIR plots of (a) AAFo-treated perovskites. Magnified FTIR plots of (b) bare and OAFo, (c) DAFo and (d) DOFo-treated perovskite films.

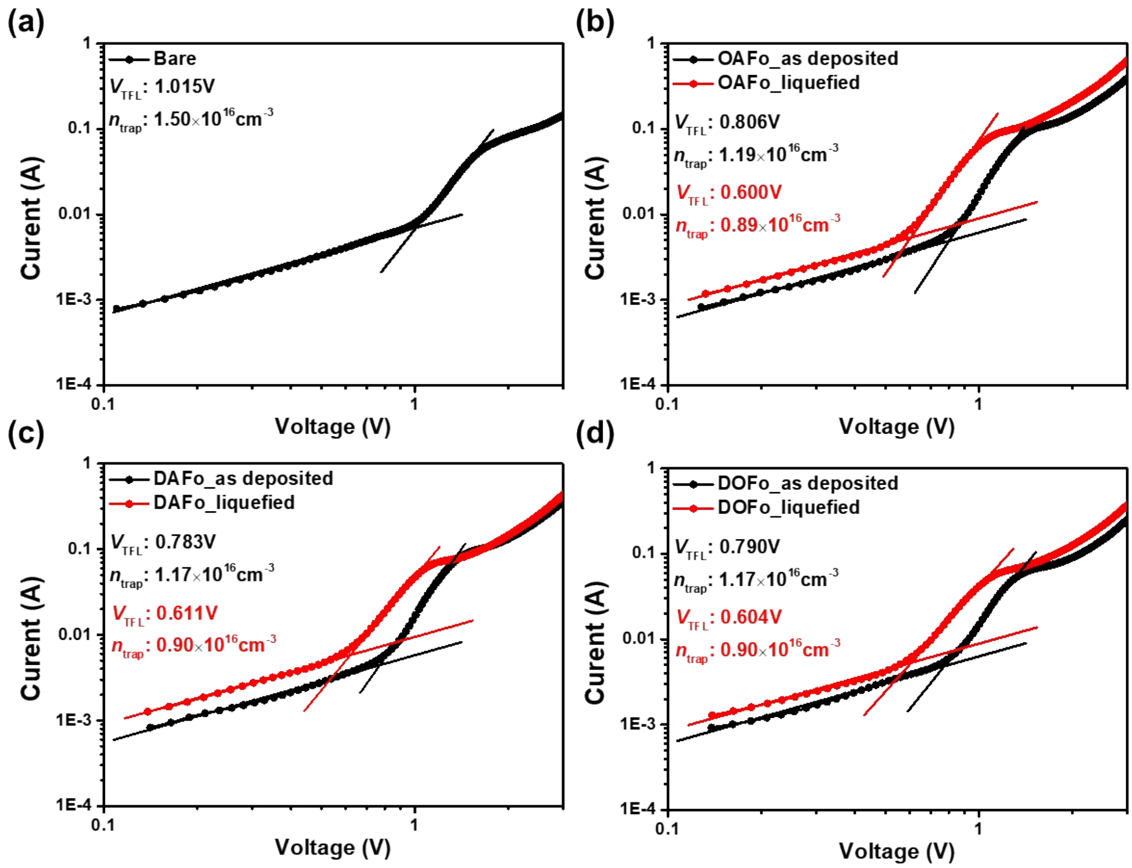

Fig. S11 SCLC plots and defect densities of the (a) bare, (b) OAFo, (c) DAFo, and (d) DOFo-treated perovskite films before and after liquid phase transition-induced passivation.

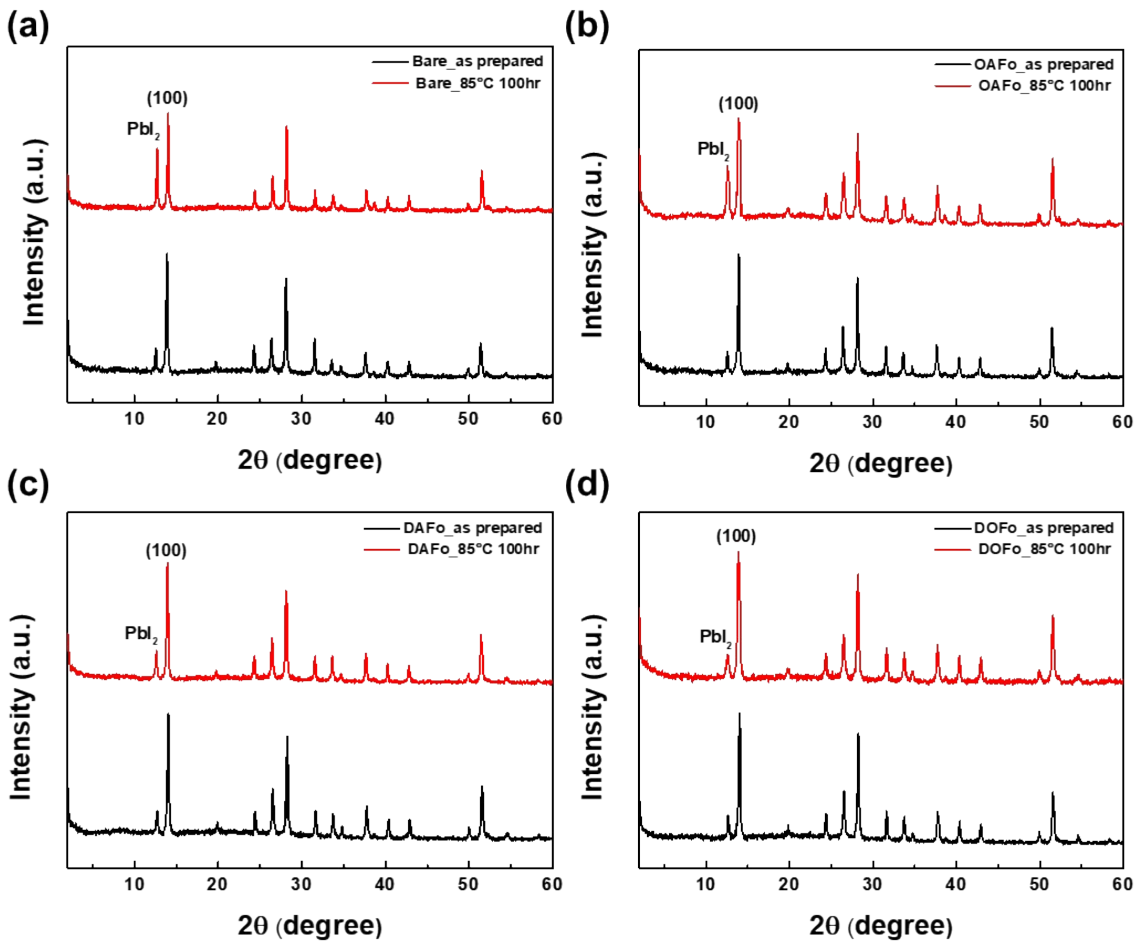

Fig. S12 XRD plots of the (a) bare, (b) OAFo, (c) DAFo and (d) DOFo-treated perovskite films before and after thermal stress (85℃ for 100 h).

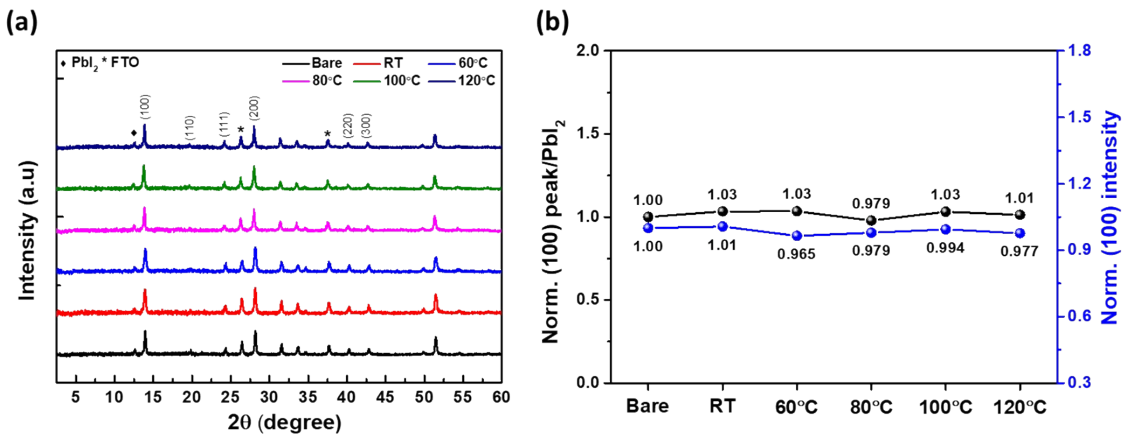

Fig. S13 (a) XRD plots of DOFo-treated perovskite films with different annealing temperatures. (b) Normalized (100) peak/PbI_2 ratio and normalized intensity of (100) peak of perovskite film with different annealing temperatures.

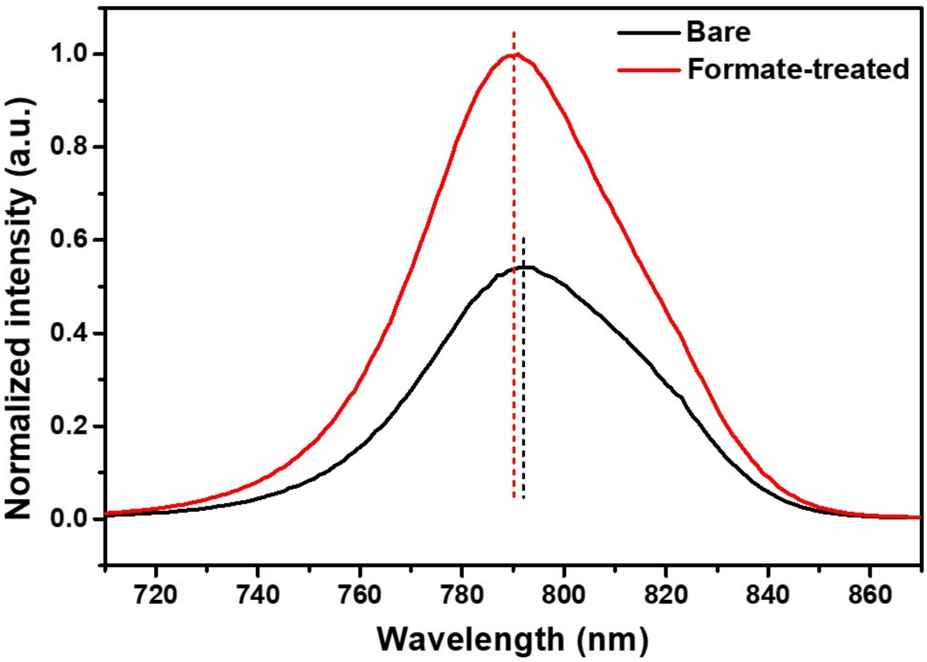

Fig. S14 Steady state photoluminescence of bare and AAFo-treated perovskite film.

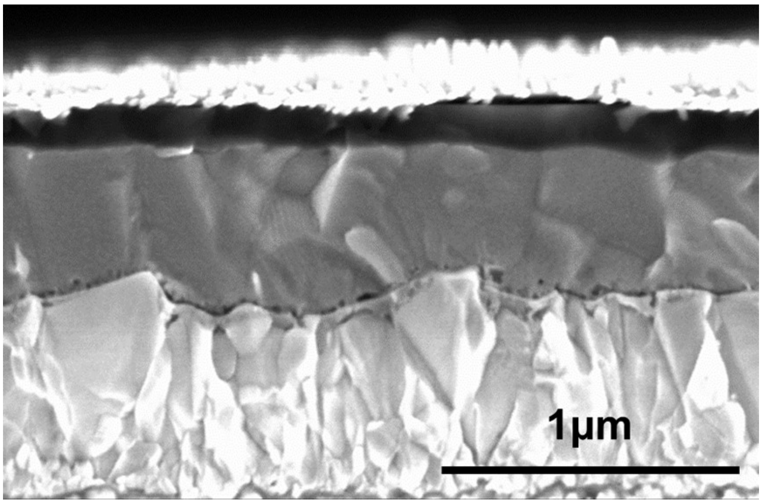

Fig. S15 Cross-sectional SEM image of formate-treated PSCs.

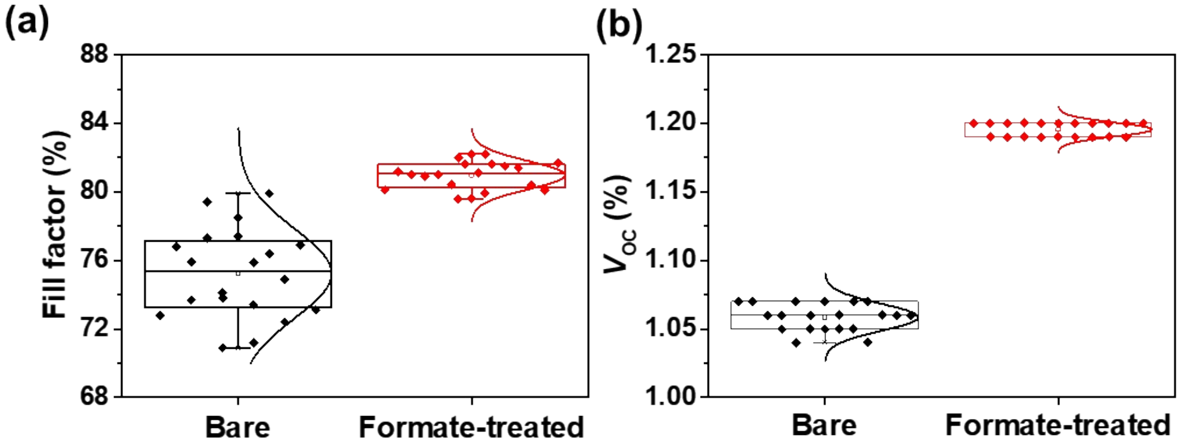

Fig. S16 Histogram of (a) fill factor and (b) V_{OC} of bare and DOFo-treated PSCs.

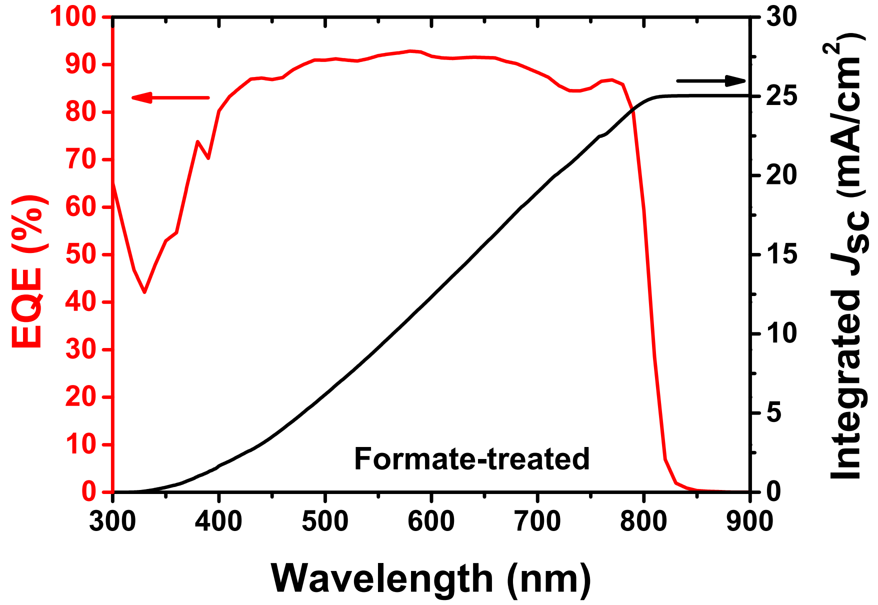

Fig. S17 External quantum efficiency (EQE) and calculated integrated J_{SC} of DOFo-treated PSC.

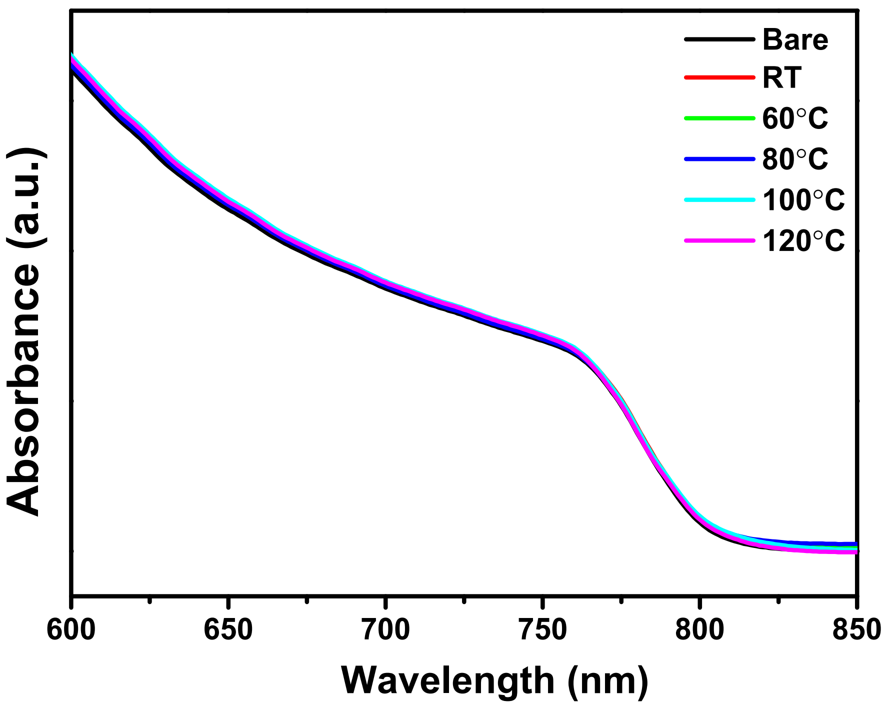

Fig. S18 UV-vis spectra of bare and DOFo-treated perovskite films with different annealing temperatures.

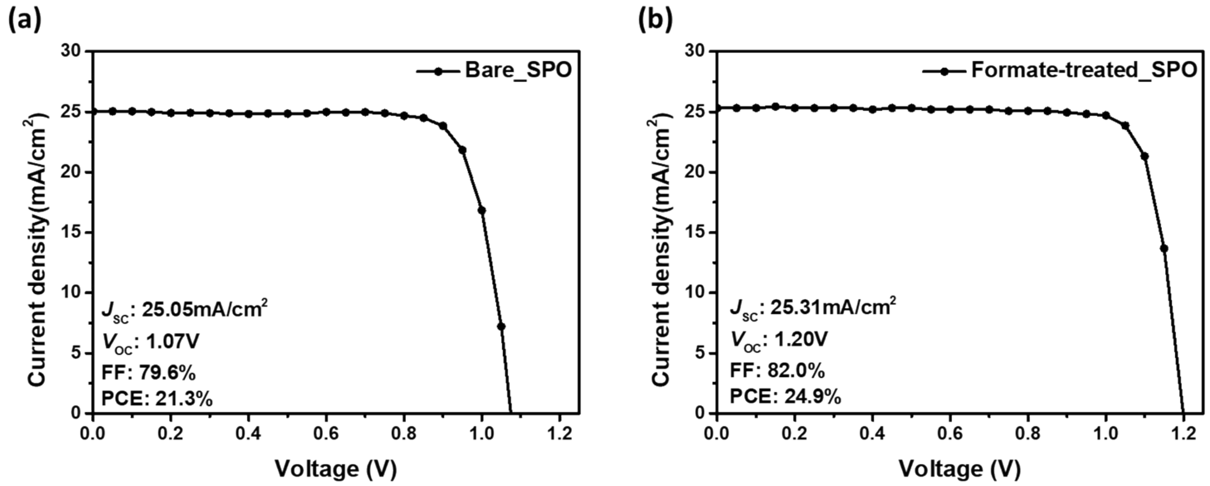

Fig. S19 *J-V* curves and device performance parameters of (a) bare and (b) DOFo-treated PSCs for SPO measurement.

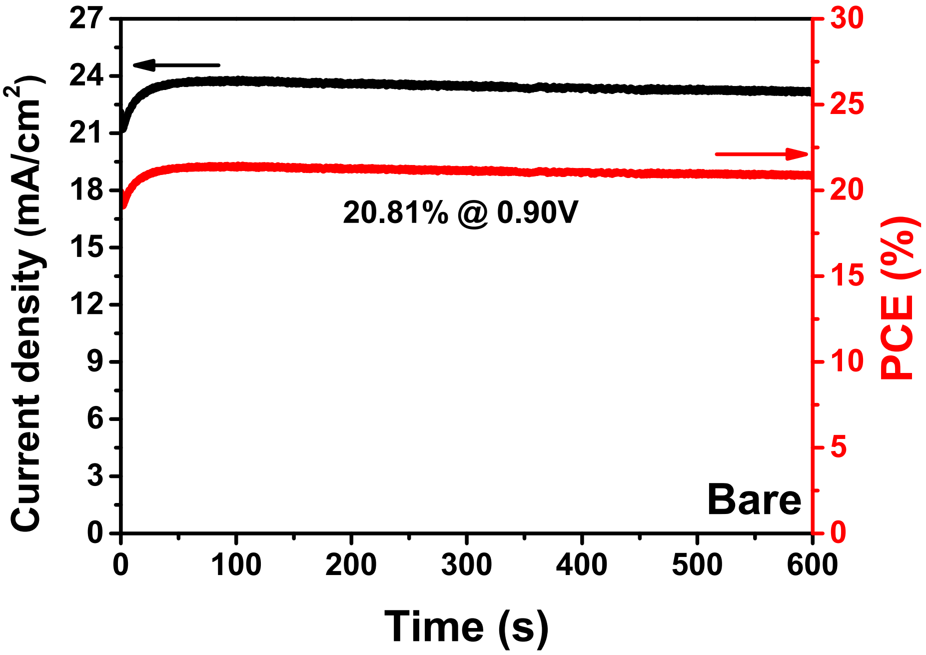

Fig. S20 Stabilized current density and power output of bare PSCs.

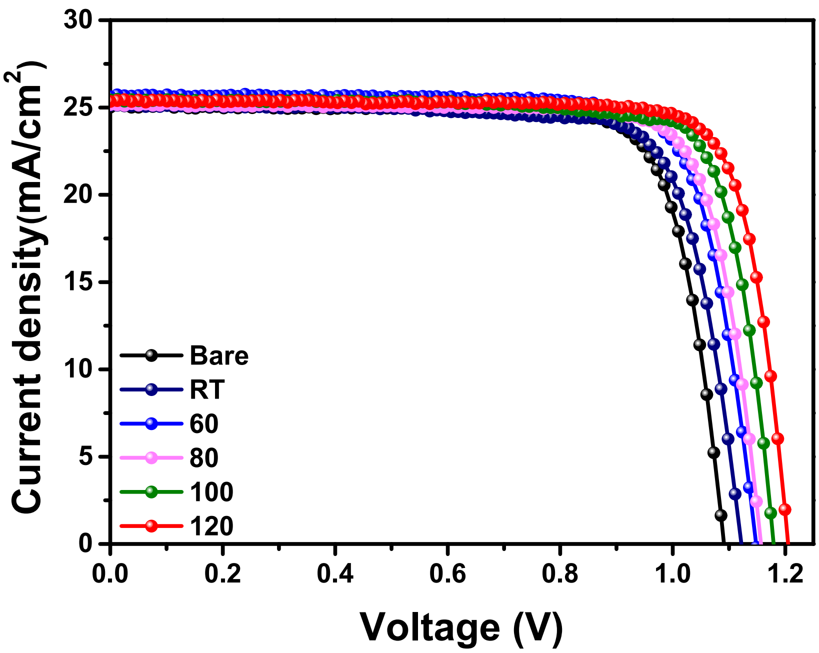

Fig. S21 *J-V* curve of best performing bare and DOFo-treated PSCs with different annealing temperatures.

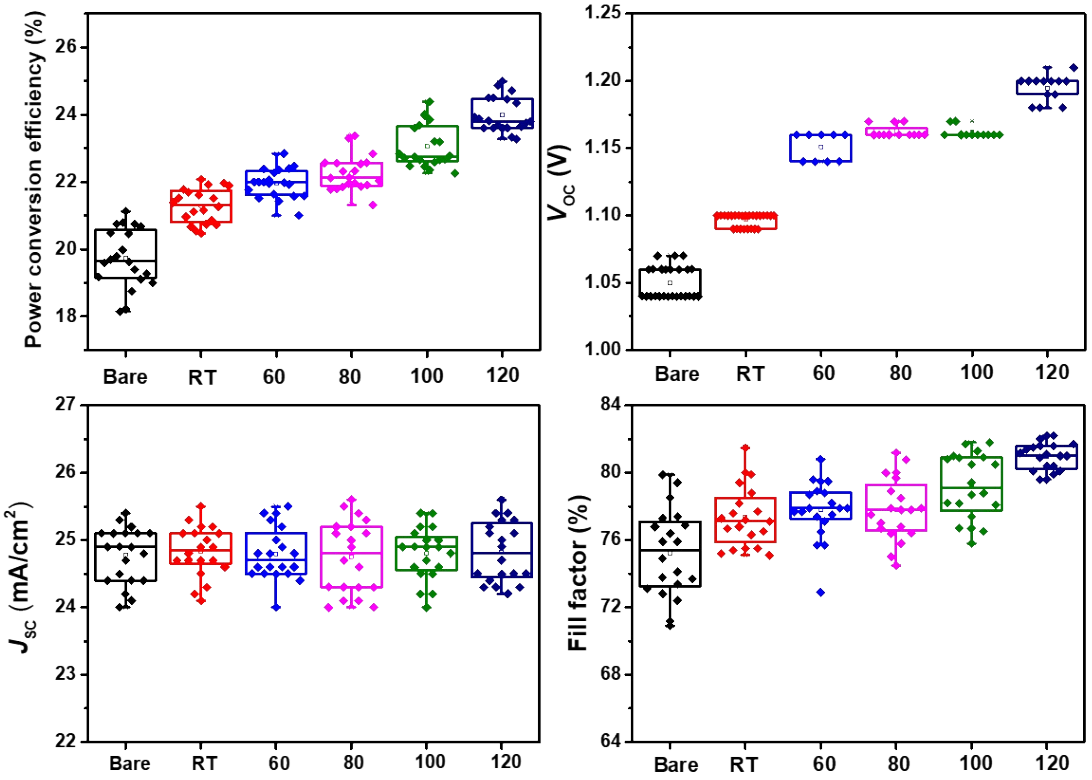

Fig. S22 Histograms of device performance parameters of bare and DOFo-treated PSCs with different annealing temperatures.

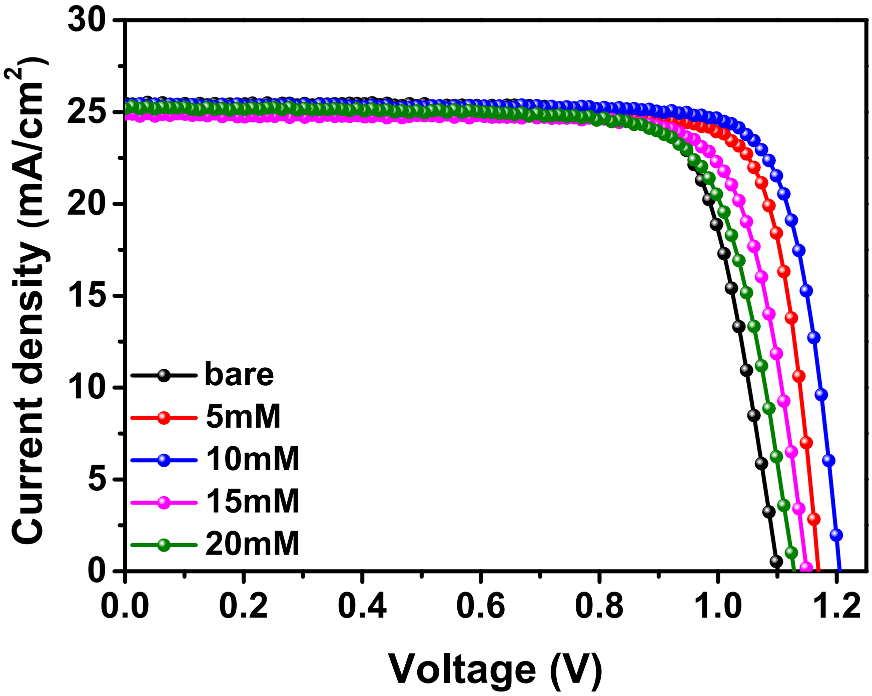

Fig. S23 *J-V* curve of DOFo-treated PSCs with different DOFo concentrations.

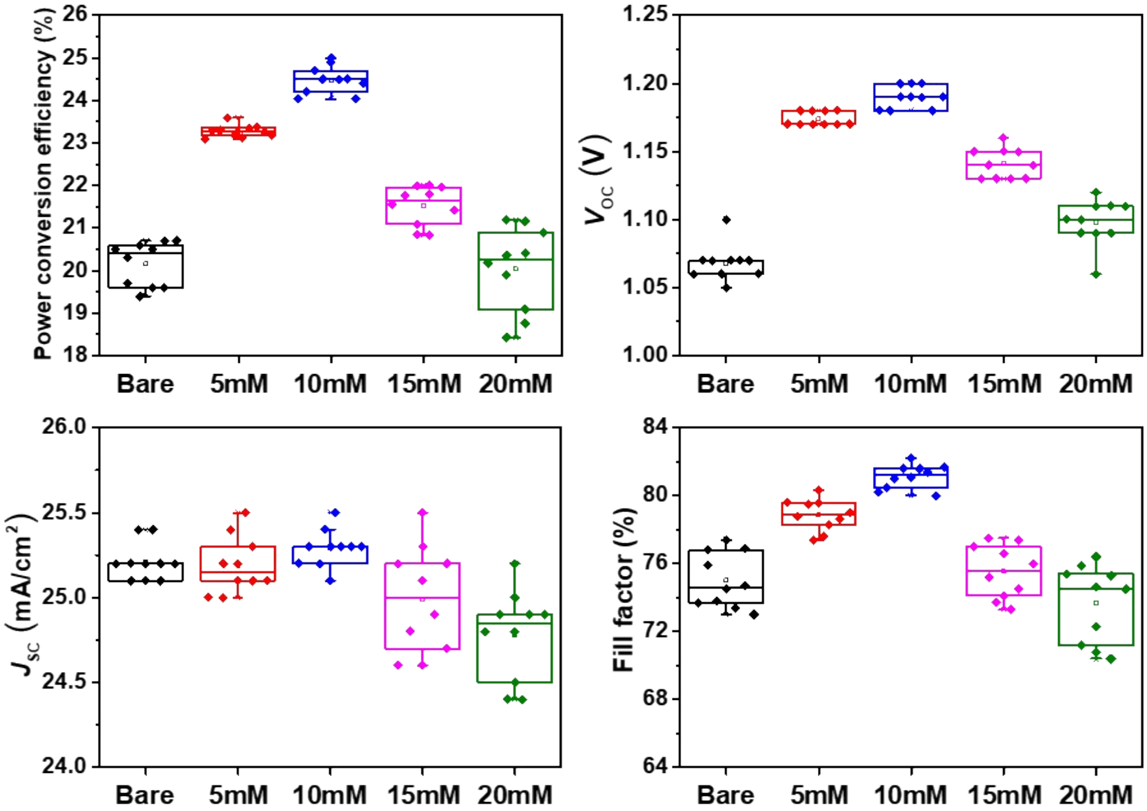

Fig. S24 Histograms of device performance parameters of DOFo-treated PSCs with different DOFo concentrations.

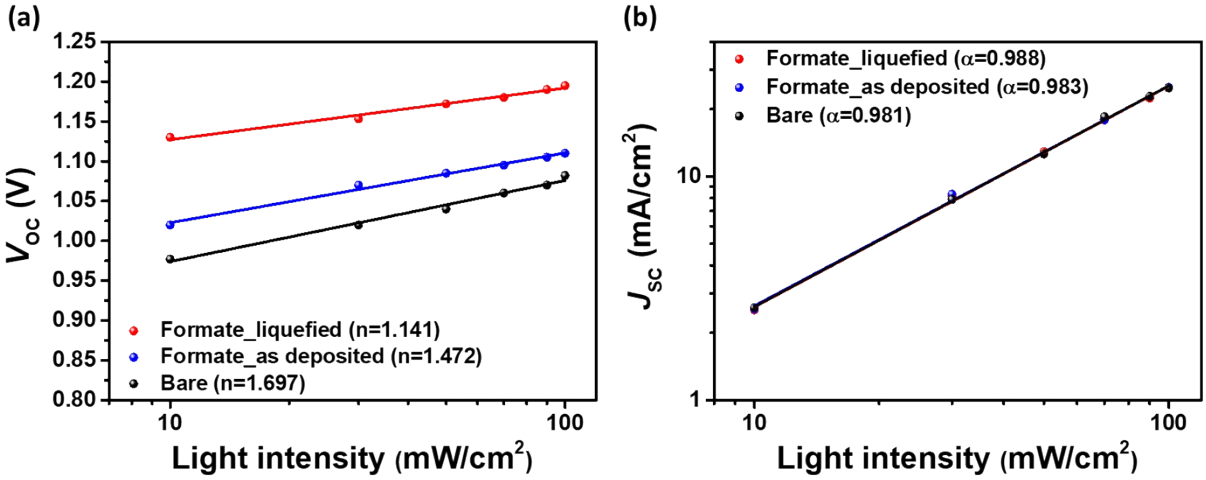

Fig. S25 Light intensity dependent (a) V_{OC} and (b) J_{SC} of bare, as-deposited DOFo and liquid DOFo-deposited PSCs.

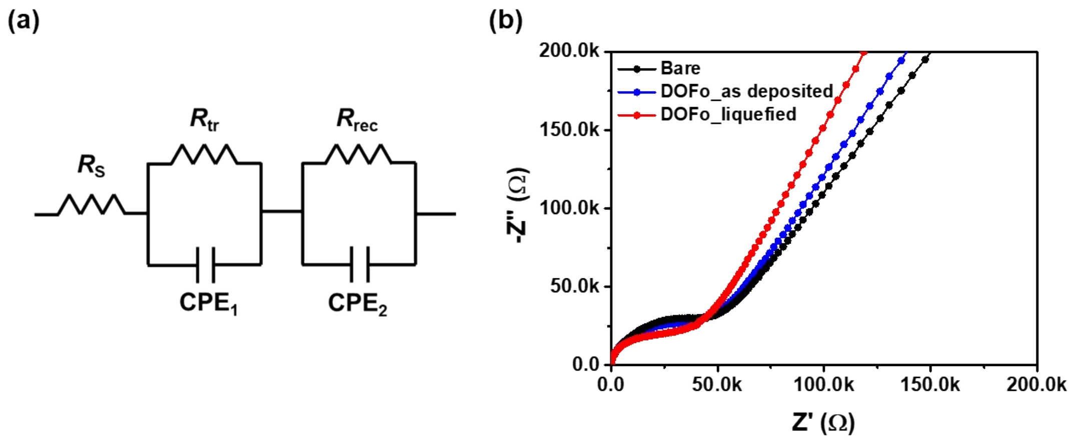

Fig. S26 (a) Equivalent circuit model for EIS measurement. (b) Nyquist plots of bare, as-deposited DOFo and liquid DOFo-deposited PSCs.

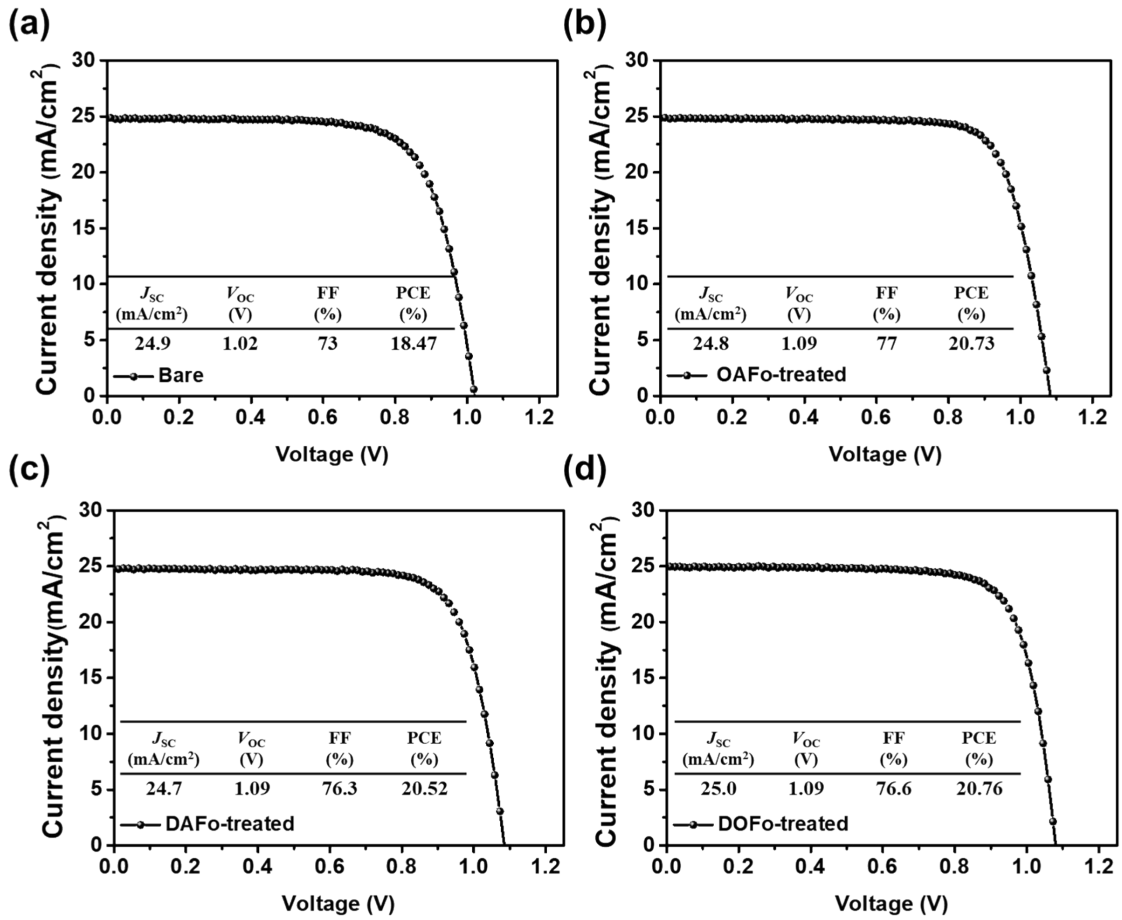

Fig. S27 *J*-*V* curves and best performing devices of (a) bare, (b) OAFo, (c) DAFo and (d) DOFo-treated PSCs using asy-PBTBDT HTL.

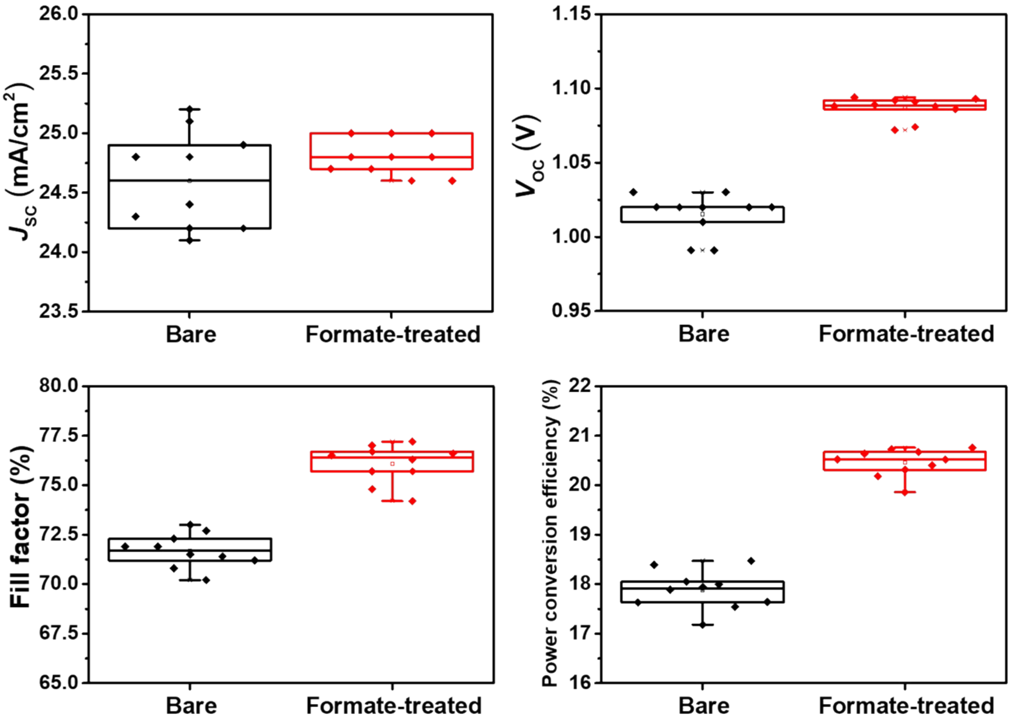

Fig. S28 Histograms of device performance parameters of bare and formate-treated PSCs using asy-PBTBDT HTL (10 devices each).

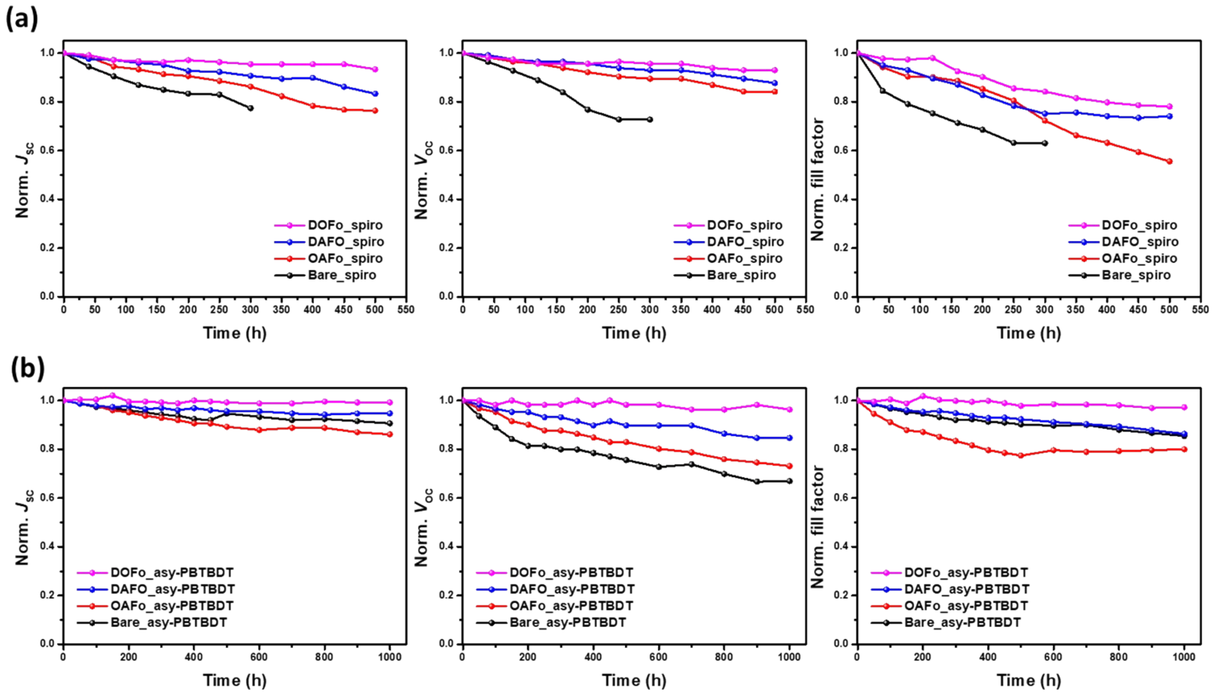

Fig. S29 Normalized device parameters of bare and AAFo-treated devices with time at the thermal conditions with (a) Spiro-OMeTAD based PSCs and (b) asy-PBTBDT based PSCs (85°C in N_2).

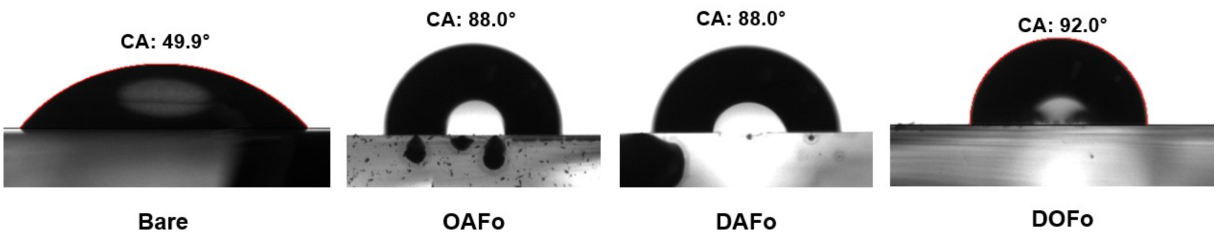

Fig. S30 Water contact angle of bare and AAFo-treated perovskite films.

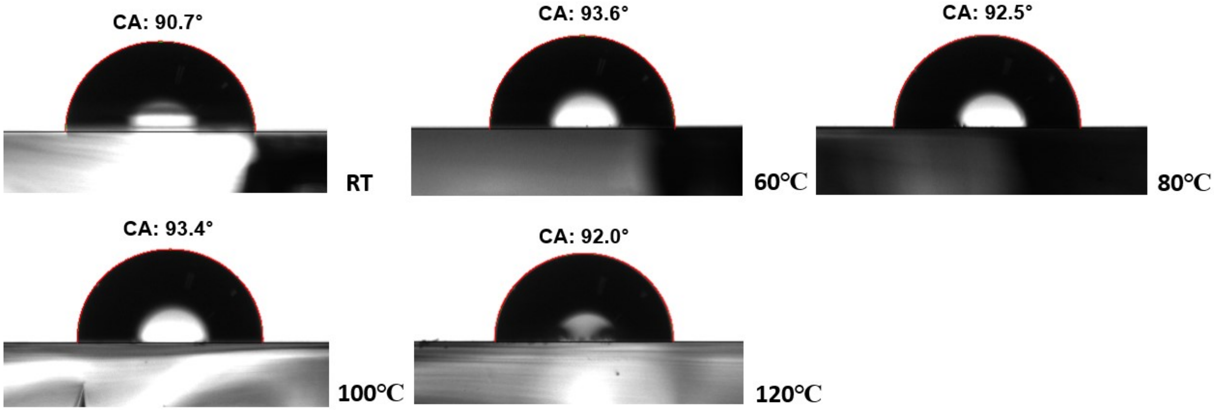

Fig. S31 Water contact angle of DOFo-treated perovskite films with different annealing temperatures.

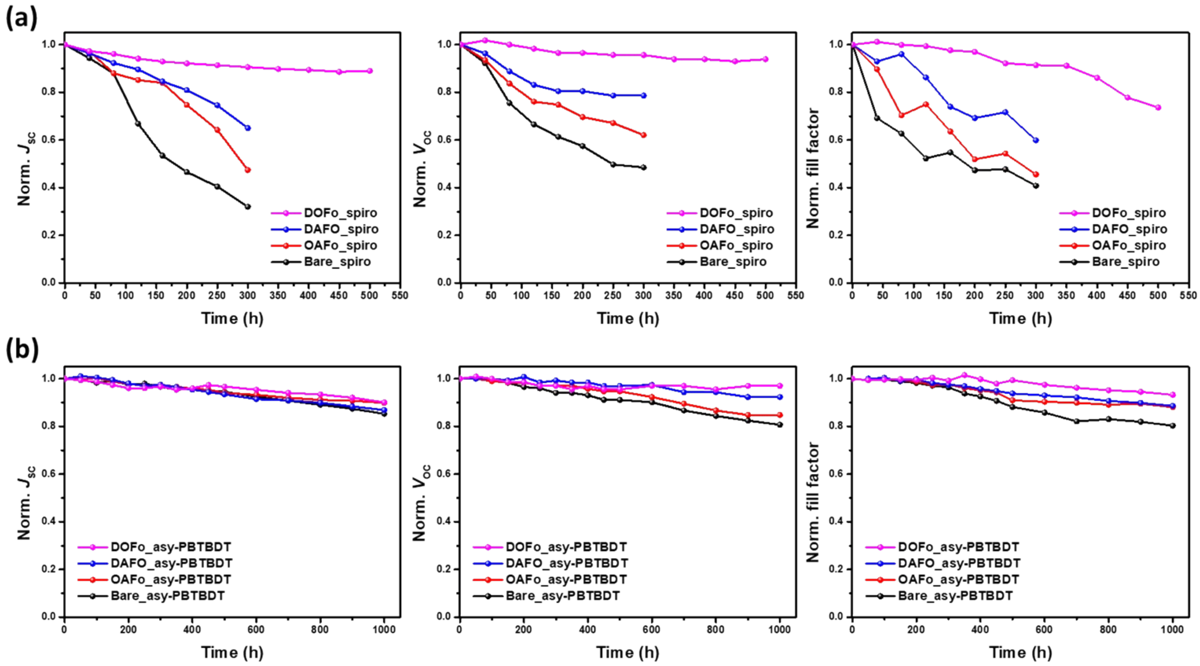

Fig. S32 Normalized device parameters of bare and AAFo-treated devices with time at the moisture condition with (a) Spiro-OMeTAD based PSCs and (b) asy-PBTBDT based PSCs (60±10 RH in RT).

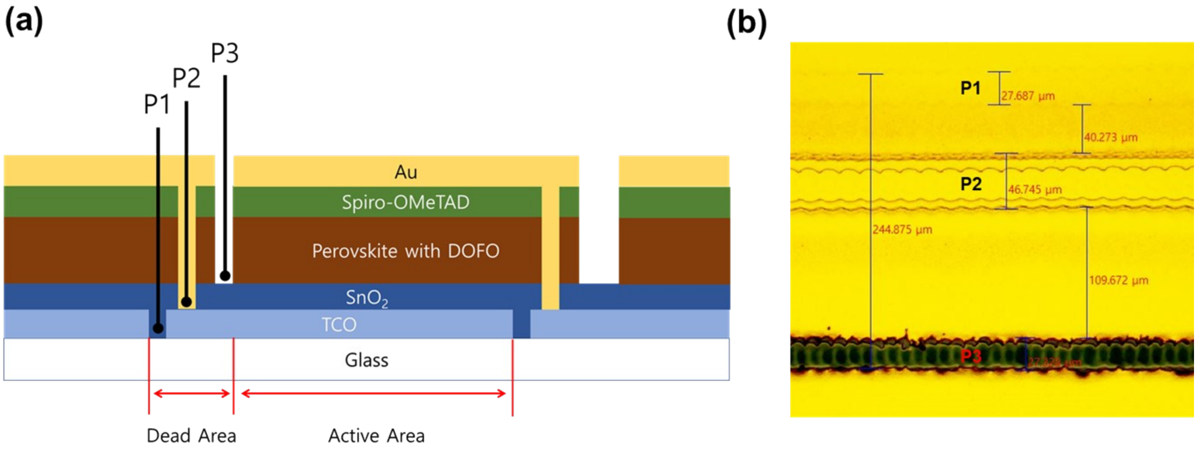

Fig. S33 (a) Schematic illustration of the perovskite module. (b) Optical image of the perovskite module.

Table S1. Summarized PL decay components of bare and AAFo-treated perovskite before and after thermal stress (85°C for 100 hours, N_2).

	τ_1 (μs)	τ_2 (μs)	A_1 (%)	A_2 (%)	τ_{avg} (μs)	**Percent change (%)**
Bare	0.0491	2.5757	27.42	72.58	2.55	**32.6**
Bare_85°C annealed	0.0535	1.7169	27.2	72.79	1.70	
OAFo	0.081	3.1836	40.47	59.5	3.13	**23.0**
OAFo_85°C annealed	0.1053	2.4962	46.4	53.6	2.41	
DAFo	0.1287	3.3218	43.28	56.72	3.23	**15.5**
DAFo_85°C annealed	0.0715	2.7789	41.79	58.21	2.73	
DOFo	0.1055	3.3268	35.13	64.84	3.27	**0.4**
DOFo_85°C annealed	0.0982	3.3179	33.25	66.71	3.26	

Table S2. Summary of V_{TFL} and n_{trap} of bare and AAFo-treated perovskite before and after thermal stress (85℃ for 100 hours, N_2).

	V_{TFL} (V)	$\boldsymbol{n_{trap}}$ **(cm^{-3})**		V_{TFL} (V)	$\boldsymbol{n_{trap}}$ **(cm^{-3})**
Bare	1.009	**1.49×10^{16}**	OAFo	0.594	**8.76×10^{15}**
Bare_85℃ annealed	1.897	**2.80×10^{16}**	OAFo_85℃ annealed	0.997	**1.47×10^{16}**
DAFo	0.622	**9.17×10^{15}**	DOFo	0.617	**9.10×10^{15}**
DAFo_85℃ annealed	0.801	**1.18×10^{16}**	DOFo_85℃ annealed	0.624	**9.20×10^{15}**

Table S3. Summary of device performance parameters of best performing devices of bare and DOFo-treated PSCs with different annealing temperatures.

	J_{SC} (mA/cm^2)	V_{OC} (V)	FF (%)	PCE (%)
Bare	25.0	1.09	76.6	20.76
RT	25.1	1.12	77.7	21.84
60℃	25.4	1.16	79.1	22.84
80℃	25.2	1.16	80.0	23.38
100℃	25.4	1.17	81.7	24.39
120℃	25.3	1.20	82.2	25.00

Table S4. The initial device performance parameters of bare and DOFo-treated PSCs with different annealing temperature (20 devices each).

	number	J_{SC} (mA/cm^2)	V_{OC} (V)	FF (%)	PCE (%)
Bare	1	24.9	1.07	73.4	19.6
	2	24.9	1.06	77.4	20.5
	3	24.4	1.06	77.3	20.0
	4	25.1	1.07	78.5	21.1
	5	25.1	1.05	73.8	19.4
	6	24.1	1.05	72.4	18.2
	7	25.1	1.05	79.4	20.8
	8	25.4	1.07	75.9	20.7
	9	24.5	1.06	79.9	20.8
	10	24.8	1.04	76.4	19.8
	11	25.1	1.07	76.8	20.7
	12	24.7	1.05	74.1	19.1
	13	24.4	1.05	71.2	18.1
	14	25.2	1.06	73.7	19.7
	15	25.1	1.06	76.9	20.5
	16	24	1.07	74.9	19.3
	17	24.4	1.06	75.9	19.6
	18	24.2	1.07	73.1	19.0
	19	25.3	1.04	70.9	18.8
	20	24.9	1.06	72.8	19.2
RT	1	25.2	1.1	76.3	21.2
	2	24.1	1.1	77.2	20.5
	3	24.7	1.1	75.5	20.5
	4	25	1.1	75.4	20.7
	5	25.3	1.1	77.6	21.6
	6	24.5	1.1	76.8	20.7
	7	24.9	1.1	79.9	21.9
	8	25.1	1.1	76.5	21.1
	9	25.1	1.1	75.5	20.9
	10	25.2	1.11	76.7	21.5
	11	24.7	1.11	78.8	21.7
	12	24.3	1.11	79.4	21.3
	13	24.7	1.1	80	21.8
	14	24.2	1.12	81.5	22.0
	15	24.8	1.12	75.2	21.0
	16	24.9	1.11	77.7	21.5
	17	25.5	1.11	77.3	21.9
	18	24.7	1.12	77.1	21.4
	19	25.1	1.12	78.2	22.1
	20	24.6	1.12	75.1	20.7

Table S4. Continued.

	number	J_{SC} (mA/cm^2)	V_{OC} (V)	FF (%)	PCE (%)
60°C	1	24.2	1.17	78.7	22.4
	2	24.9	1.17	76.7	22.5
	3	24.2	1.17	79.4	22.6
	4	24	1.17	80.5	22.7
	5	25	1.17	81.3	23.9
	6	24.5	1.18	78.2	22.7
	7	25.4	1.17	81.7	24.4
	8	24.7	1.17	78.8	22.8
	9	25.4	1.18	75.8	22.7
	10	24.9	1.18	81.8	24.0
	11	25.2	1.18	80.9	24.0
	12	24.6	1.17	78.2	22.5
	13	25.1	1.18	76.7	22.8
	14	24.9	1.17	78.1	22.7
	15	24.5	1.17	80.9	23.2
	16	25	1.17	80.8	23.7
	17	24.6	1.17	80.5	23.2
	18	24.9	1.17	76.5	22.3
	19	24.8	1.17	81	23.6
	20	25.2	1.17	77.4	22.8
80°C	1	24.6	1.13	77.1	21.4
	2	24.6	1.14	79.5	22.4
	3	25	1.13	76.5	21.6
	4	24.5	1.14	79.6	22.3
	5	25.4	1.14	78.8	22.8
	6	24	1.14	80.8	22.1
	7	25.4	1.14	75.7	22.0
	8	25.5	1.14	77.4	22.4
	9	24.9	1.14	77.5	21.9
	10	24.8	1.14	77.9	21.9
	11	24.8	1.14	77.9	22.0
	12	24.5	1.13	77.7	21.6
	13	25.2	1.13	75.7	21.5
	14	24.6	1.14	79.5	22.4
	15	24.6	1.15	78.9	22.5
	16	25.3	1.14	72.9	21.0
	17	24.8	1.14	77.9	22.0
	18	24.5	1.13	77.7	21.6
	19	24.5	1.14	78.2	21.8
	20	24.4	1.14	78.7	22.0

Table S4. Continued.

	number	J_{SC} (mA/cm^2)	V_{OC} (V)	FF (%)	PCE (%)
100°C	1	25.2	1.16	80	23.4
	2	25	1.16	76.8	22.3
	3	24.3	1.16	77.8	22.0
	4	25.2	1.16	79.7	23.3
	5	24.1	1.15	80	22.1
	6	24.1	1.15	81.2	22.5
	7	24.6	1.16	77.9	22.3
	8	25.1	1.15	76.4	22.0
	9	25.4	1.16	76.4	22.6
	10	24.3	1.15	80.8	22.6
	11	24.3	1.15	77.8	21.9
	12	24	1.16	78.5	21.9
	13	24.7	1.15	77	21.9
	14	24.3	1.15	77.9	21.8
	15	24	1.15	77.5	21.3
	16	25.1	1.15	78.9	22.8
	17	24.9	1.15	75.8	21.8
	18	25.5	1.16	74.5	22.1
	19	25.6	1.15	75	22.0
	20	25.3	1.16	76.7	22.6
120°C	1	25.3	1.2	82.2	25.0
	2	25.6	1.2	81.1	24.9
	3	25.2	1.19	81.6	24.5
	4	25.3	1.19	81.6	24.5
	5	24.9	1.2	80.5	23.9
	6	24.2	1.2	81.5	23.7
	7	25.4	1.2	81	24.7
	8	25.4	1.19	81.4	24.5
	9	24.7	1.2	79.6	23.6
	10	24.3	1.2	80.9	23.6
	11	25.2	1.2	78.3	23.6
	12	24.5	1.2	81	23.8
	13	25.7	1.2	81.2	25.0
	14	25	1.19	79.6	23.6
	15	24.3	1.19	82	23.7
	16	24.5	1.2	81.2	23.9
	17	24.3	1.19	82.2	23.8
	18	25.1	1.19	81.7	24.4
	19	24.9	1.2	80.1	23.9
	20	25.1	1.19	79.9	23.8

Table S5. Summary of device performance parameters of best performing devices of DOFo-treated PSCs with different DOFo concentrations (10 devices each).

	J_{SC} (mA/cm^2)	V_{OC} (V)	FF (%)	PCE (%)
Bare	25.4	1.07	75.9	20.7
Formate_5mM	25.1	1.17	80.3	23.6
Formate_10mM	25.3	1.2	82.2	25
Formate_15mM	24.9	1.14	77.5	22.0
Formate_20mM	25.2	1.11	75.4	21.2

Table S6. The initial device performance parameters of DOFo-treated PSCs with different DOFo concentrations (10 devices each).

	number	J_{SC} (mA/cm^2)	V_{OC} (V)	FF (%)	PCE (%)
Bare	1	24.9	1.07	73.4	19.6
	2	24.9	1.06	77.4	20.5
	3	25.1	1.05	73.8	19.4
	4	25	1.07	73	19.6
	5	25.2	1.1	74.5	20.6
	6	25.4	1.07	75.9	20.7
	7	25.4	1.07	74.7	20.3
	8	25.1	1.07	76.8	20.7
	9	25.2	1.06	73.7	19.7
	10	25.1	1.06	76.9	20.5
5mM	1	25.5	1.17	77.6	23.12
	2	25.4	1.18	77.4	23.19
	3	25.1	1.17	79.6	23.35
	4	25.1	1.17	80.3	23.59
	5	25.2	1.17	79.5	23.38
	6	25.3	1.18	78.3	23.3
	7	25	1.18	78.8	23.26
	8	25.1	1.18	78.6	23.29
	9	24.9	1.17	79.6	23.18
	10	25	1.17	79	23.1
10mM	1	25.3	1.2	82.2	25
	2	25.6	1.2	81.1	24.9
	3	25.2	1.19	81.6	24.5
	4	25.3	1.19	81.6	24.5
	5	25.4	1.2	81	24.7
	6	25.4	1.19	81.4	24.5
	7	25.4	1.18	80.5	24.2
	8	25.4	1.18	80	24.04
	9	25.3	1.18	80.2	24.03
	10	25.1	1.19	81.7	24.4
15mM	1	24.6	1.16	73.3	20.84
	2	24.6	1.15	76.6	21.79
	3	24.9	1.14	77.5	22.01
	4	24.7	1.15	74.1	21.09
	5	25.3	1.15	75.2	21.96
	6	24.8	1.14	73.7	20.85
	7	25.2	1.13	77.4	22
	8	25.1	1.13	77	21.76
	9	25.5	1.13	74.5	21.42
	10	25.2	1.13	76	21.56
20mM	1	24.8	1.11	74.6	20.41
	2	24.4	1.1	75.9	20.36
	3	24.9	1.11	76.4	21.16
	4	24.4	1.09	70.8	18.76
	5	24.5	1.06	71.2	18.43
	6	24.9	1.09	70.4	19.09
	7	24.8	1.12	75.3	20.9
	8	25	1.1	72.3	19.9
	9	25.2	1.11	75.4	21.19
	10	24.9	1.09	74.5	20.18

Table S7. Summary of calculated EIS parameters from Nyquist plots of bare and DOFo-treated PSCs with and without phase transition.

	R_{tr} (Ω)	CPE_1 (F)	R_{rec} (Ω)	CPE_2 (F)
Bare	64961	20.33E-9	1.68E6	0.39E-6
DOFo_as deposited	55496	35.66E-9	2.36E6	0.43E-6
DOFo_liquefied	38146	40.93E-9	3.59E6	0.53E-6

Table S8. Comparison of area, PCE and fill factor of small and large-area devices obtained in this work with those recently reported in literatures (planar PSCs with SnO_2 and Spiro-OMeTAD).

Device structure	**Small-area**		**Large-area (module)**			**reference**
	Area [cm^2]	PCE [%]	Area [cm^2]	PCE [%]	Fill factor [%]	
FTO/SnO_2/$GA_{0.12}MA_{0.88}PbI_3$/Spiro-OMeTAD/Au	0.125	19.44	16	13.85	71.2	D.-K. Lee et al., *ACS Energy Lett.*, 2019, **4**, 2393.
FTO/SnO_2/$(CsPbI_3)_{0.05}[(FAPbI3)_{0.85}(MAPbBr_3)_{0.15}]_{0.95}$/Spiro-OMeTAD/Au	0.14	19.4	25/100	15.3/ 14.03	69/68	G. S. Han et al., *ACS Energy Lett.*, 2019, **4**, 1845.
FTO/SnO_2/$Cs_{0.06}MA_{0.27}FA_{0.67}PbI_{2.7}Br_{0.3}$/Spiro-OMeTAD/Au	0.09	17.81	22.8	12.03	61.3	L. Qiu et al., *Adv. Funct. Mater.*, 2019, **29**, 1806779.
FTO/SnO_2/$Cs_{0.05}FA_{0.54}MA_{0.41}Pb(I_{0.98}Br_{0.02})_3$/Spiro-OMeTAD-P3HT/Au	0.09	20.1	22.4	16.6	72.9	Z. Liu et al., *Nat. Energy*, 2020, **5**, 596.
FTO/SnO_2/C_{60}/$(CsPbI_3)_{0.05}((FAPbI_3)_{1-x}(MAPbBr_3)_x)_{0.95}$/Spiro-MeOTAD/Au	0.188	21.95	25.49	17.88	78.6	A. Ren et al., *Joule*, 2020, **4**, 1263–1277
FTO/SnO_2/$MAPbI_3$/Spiro-OMeTAD/Au	0.16	20.28	21	18.13	73.4	J. Li et al., *Joule*, 2020, **4**, 1035.
FTO/SnO_2/$FA_{0.83}Cs0_{.17}PbI_3$/Spiro-OMeTAD/Au	0.148	23.35	17.1/65	20.42/ 19.54	78.1/ 76.1	T. Bu et al., *Science*, 2021, **372**, 1327.
FTO/SnO_2/$Cs_{0.03}FA_{0.97}PbI_3$/Spiro-OMeTAD/Au	0.12	20.48	16/ 100	16.69/ 13.84	71.11/ 58.01	R. Chen et al., *Adv. Funct. Mater.*, 2021, **31**, 2008760
FTO/SnO_2/$Cs_{0.05}FA_{0.85}MA_{0.10}PbI_{2.85}Br_{0.15}$/Spiro-OMeTAD/Au	0.09	21.7	22.4	17.26	69.9	G. Tong et al., *Nano-Micro Lett.*, 2021, **13**, 155.
FTO/SnO_2/$Cs_{0.03}FA_{0.97}PbI_3$/Spiro-OMeTAD/Au	0.12	22.06	36	18.1	70.94	R. Chen et al., *J. Am. Chem. Soc.*, 2021, **143**, 10624–10632
FTO/SnO_2/$Cs_{0.15}FA_{0.85}PbI_{2.85}Br_{0.05}Cl_{0.1}$/Spiro-MeOTAD/Au	0.09	23	10.3	19.3	71.3	Z. Fan et al., *Chem. Sci.*, 2022, **13**, 10512
FTO/SnO_2/$FA_{0.95}MA_{0.05}PbI_{2.85}Br_{0.15}$/Spiro-MeOTAD/Au	0.148	24.4	10	20.4	73	Y. Wang et al, *Adv. Funct. Mater.*, 2022, **32**, 2204396
FTO/SnO_2/$(FAPbI_3)_{0.85}(MAPbBr_3)_{0.15}$/Spiro-MeOTAD/Au	0.891	21.0	30.24	19.06	77.0	S. D.-Geguziene et al, *Angew. Chem. Int. Ed.*, 2022, **61**, e202113207
FTO/SnO_2/$FA_{0.8}Cs_{0.2}PbI_{2.4}Br_{0.6}$/Spiro-OMeTAD/au	0.16	19.8	10	17.0	76	X. Ma et al., *Chem. Eng. J.*, 2022, **445**, 136626
FTO/SnO_2/$Cs_{0.05}FA_{0.85}MA_{0.10}Pb(I_{0.97}Br_{0.03})_3$/PEAI/Spiro-OMeTAD/Au	0.09	18.94	57.5	16.22	64.86	P. J. S. Rana et al., *Adv. Funct. Mater.*, 2022, **32**, 2113026.
ITO/SnO_2/$FA_{0.92}MA_{0.08}PbI_3$/Spiro-OMeTAD/au	0.09	23.27	19.32	15.31	68.43	Y. Hu et al., *Small Methods*, 2022, **6**, 210125
ITO/SnO_2/FPAC60/PVSK(bis-DMEC60)/Spiro-OMeTAD/Au	1.0	22.58	17.11	19.53	75.8	S. Zhang et al., *ACS Energy Lett.*, 2022, **7**, 11, 3958–3966

ITO/SnO_2/$Cs_{0.05}FA_{0.85}MA_{0.10}Pb(I_{0.97}Br_{0.03})_3$/Spiro-OMeTAD/Au	1.0	23.5	17.1	21.4	79.2	S. You et al., *Science*, 2022, **379**, 288–294
ITO/SnO_2/$Cs_{0.1}FA_{0.9}PbI_3$/Spiro-OMeTAD/Au	0.12	24.3	18	19.61	75.39	R. Chen et al., *Adv. Sci.*, 2022, **9**, 2204017
FTO/SnO_2/$FA_{0.95}MA_{0.05}PbI_{2.85}Br_{0.15}$/Spiro-OMeTAD /Au	0.148	24.4	10/15	20.4/ 18.1	70.3/ 70.4	Y. Wang et al., *Adv. Funct. Mater.*, 2022, **32**, 2204396
FTO/SnO_2/perovskite/CL/Spiro-OMeTAD/Au	0.1	24.43	10.75	20.33	76.67	X. Zhu et al., *Adv. Energy Mater.*, 2022, **12**, 2103491
FTO/SnO_2/$(FAPbI_3)_{0.97}(MAPbBr_3)_{0.03}$/Spiro-OMeTAD/Au	**0.09**	**25**	**23.75 /25**	**20.82/ 19.78**	**80.77**	**This work**

*The black letters indicate the value based on the active area standard and the red letters indicate the value based on the aperture area standard.